Fluorescence Spectroscopic Studies of (Amide + Electrolyte) Deep Eutectic Systems

Biswajit Guchhait and Ranjit Biswas*

Department of Chemical, Biological and macromolecular Sciences, S. N. Bose National Centre for Basic Sciences, Block-JD, Sec-III, Salt Lake, Kolkata – 700098
*E-mail: ranjit@bose.res.in

Abstract

Steady state and time-resolved fluorescence measurements have been carried out for deep eutectic (acetamide + electrolyte) molten mixtures in the temperature range, ~303 – 348 K. These measurements indicate presence of pronounced medium heterogeneity in solution structure and viscosity decoupling of solute solvation and rotation rates. These results are reminiscent of findings in deeply supercooled liquids near glass transition.

Keywords: deep eutectic solvents, fluorescence measurements, viscosity decoupling

Refs: ISRAPS Bulletin, volm. 25, pages 31-39, 2013

I. Introduction:

Room temperature Ionic liquids [1] and supercritical fluids[2] are the rapidly growing field of research because they have attracted considerable attention as reaction media that can replace common organic solvents which are volatile and hazardous. Mixtures of amides and metal salts [3] are another set of alternative media whose properties could be tailored by changing mixture compositions and temperature. Eventhough the constituent species of such mixtures melts at temperature much above room temperature, upon mixing at certain proportion they form liquid at or near room temperature. These systems are known as deep eutectic solvents (DES) and exhibit a huge depression of freezing point due to interaction between constituent components. [4]

We are interested in solution structure and dynamics of DES composed of simple organic amides and inorganic salts because of their application as reaction media.[5,6] Conventional ionic liquid show hydrogen bonding, therefore possess a structural directionality but molten salts do not exhibit such hydrogen bonding except ionic bond. However, like in ionic liquids, DES composed of acetamide and electrolyte also exhibit hydrogen bonding. Therefore, weak interactions may have different effects on the structure of both ionic liquids and DES. Similar to ionic liquids, these DES composed of organic dipolar species (amide) and inorganic ions (electrolyte). Both DES and ionic liquids are very interesting systems because of striking deviation found in chemical and physical properties in comparison to common solvents.[5-7] These deviations are attributed to longer-ranged electrostatic interactions and are proportional to r^{-1}, r^{-2} and r^{-3}, r being the distance between two interacting species.

These DES possess various interesting properties such as high conductivity, nonvolatility, high thermal stability and large electrochemical window.[5,6,8] Because of these favourable solvent properties DES have potentials in electrochemical devices, supercapacitor technology [9] and as a media for synthesis of semiconducting films and nanomaterials [10]. Recently, it has been observed that these deep eutectic mixtures can be used as an excellent electrolyte to improve the efficiency of battery [11]. The present DES can easily be prepared by mixing short chain amides and electrolytes at suitable proportions. Their physico-chemical properties can be monitored by varying the cation and anion of constituent electrolyte, and alkyl chain

length and functional group of amide. Moreover the constituent components for these DES are available at low cost compared to common ionic liquids. Therefore the ease of preparation, availability and various important applications make these new classes of solvents possible alternatives to room temperature ionic liquids.

Nuclear Magnetic resonance spectroscopic measurement[12] of the fluorinated amide and electrolyte system has confirmed that the amide and salt participate in different environments, the amide environment being less rigid. These systems are therefore micro-heterogeneous in nature. Interestingly, while a lot of concern has been devoted to investigate the structure and dynamics of ionic liquids[13-16], similar attention has been missing for these DES. Therefore, these systems need thorough investigation in order for better and smarter application of them as reaction media.

Of late, we have applied steady state and time resolved fluorescence spectroscopy to get an idea of structure and dynamics of these DES [17-20]. We have studied solvent and solute relaxation of a dipolar solute, coumarin 153 (C153) in various DES composed of acetamide (CH_3CONH_2) with various inorganic salts ~ 100 K above glass transition temperature (T_g). These studies reveal several interesting results regarding structure and dynamics of DES. Our studies on DES composed of CH_3CONH_2 with sodium/potassium thiocyanates (Na/KSCN) and lithium nitrate/bromide ($LiNO_3$/Br) revealed strong excitation wavelength dependence and a fractional viscosity dependence of both average solvation ($<\tau_s>$) and rotational relaxation ($<\tau_r>$) times of the dissolved dipolar solute. A short of decoupling between rotation and translation has also been found which is similar to what has been observed in strongly supercooled liquids. In other word, Stokes-Einstein (SE) and Stokes-Einstein-Debye (SED) relations are not able to quantitatively describe the diffusive relaxation in these media. This deviation from normal SE and SED behavior is explained in terms of spatio-temporal heterogeneity of these media. In contrast, ionic liquids nearly follow the hydrodynamics, eventhough, they posses heterogeneity. In this bulletin, we will summarize our recent results obtained from the studies on (amide + electrolyte) DES, where dependence of medium heterogeneity on the ion identity and alkyl chain length will also be discussed.

II. **Experimental Section:**

Laser grade C153 was obtained from Exciton and used as received. CH_3CONH_2, NaSCN, and $LiNO_3$ were purchased from SRL, India. KSCN and LiBr were obtained from Merck Propionamide ($CH_3CH_2CONH_2$), butyramide ($CH_3CH_2CH_2CONH_2$) and Lithium perchlorate ($LiClO_4$) were received from Sigma-Aldrich. All these chemicals were used without further purification. Three sets of DES, [$0.75CH_3CONH_2$ + $0.25\{f$KSCN + $(1-f)$KSCN$\}$], [$0.78CH_3CONH_2$ + $0.22\{f$LiBr + $(1-f)LiNO_3\}$] and [$0.81CH_3CONH_2$ + $0.19LiClO_4$] have been prepared. The details regarding sample preparation have been described elsewhere [17,19,20]. The concentration of the C153 probe was kept in the range of 10^{-6} M in samples. Steady-state absorption and emission spectra were recorded using a Shimadzu UV-2450 spectrophotometer and Jobin Yvon Fluoromax-3 fluorimeter respectively. Time-resolved fluorescence measurements were carried out using a time correlated single-photon-counting (TCSPC) spectrometer from LifeSpec-ps, Edinbourg, U.K. In the present work, 409 nm pulse laser was used as the excitation source. In our TCSPC setup the instrument response function (IRF) was ~ 70 ps at full width at half maximum. For temperature dependent experiments, we regulated the temperature with an attachment from Julabo (Model: F32). For solvation dynamics studies, fluorescence intensity decays were collected at the magic angle (54.7°) with respect to vertically polarized excitation. Time-resolved emission spectra (TRES) were constructed from a set of decays obtained at different wavelengths covering the entire emission band of the C153 [21]. From the peak position of the TRES, solvation response functions, $S(t)$ were constructed and defined as $S(t) = \{\nu(t) - \nu(\infty)\}/\{\nu(0) - \nu(\infty)$, where $\nu(0)$, $\nu(t)$, and $\nu(\infty)$ are the frequencies of the emission maxima at times 0, *t*, and ∞, respectively. The above method for the construction of TRES and $S(t)$ have been discussed in detail elsewhere[17-21]. The $S(t)$ curve represents solvent in response to photo-excitation of the solute. Measured $S(t)$ decays were found to fit to bi-exponential functions of time. Finally, the average solvatione time, $< \tau_s >$, was obtained from the amplitudes (a_i) and time constants (τ_i) of the bi-exponential fitting, $\langle \tau_s \rangle = \sum_{i=1}^{2} a_i \tau_i$.

For anisotropy studies, we used the same experimental setup, fluorescence decays with parallel $\{I_{\parallel}(t)\}$, perpendicular $\{I_{\perp}(t)\}$ and magic angle polarizations with respect to that of the vertically polarized excitation of the solute were collected. The magic angle decay was

first deconvoluted from the IRF and fitted to multi-exponential function of time. Subsequently, parallel $\{I_{\parallel}(t)\}$ and perpendicular $\{I_{\perp}(t)\}$ decays were simultaneously fitted by using an iterative reconvolution algorithm[22]. Time resolved fluorescence anisotropy, $r(t)$ was constructed as $r(t) = \{I_{\parallel}(t) - GI_{\perp}(t)\}/\{I_{\parallel}(t) + 2GI_{\perp}(t)\}$, where G is a correction factor for the polarization bias of the detection setup. The average value of G was found to be 1.17 ± 0.05. A bi-exponential function of time was used to fit the obtained $r(t)$ as $r(t) = r(0)[a_1 \exp(-t/\tau_1) + (1-a_1)\exp(-t/\tau_2)]$ where τ_i (i = 1, 2) represents the time constants for the decay components (a_i). Tri or stretched exponentials did not describe the constructed $r(t)$ as good as by the bi-exponentials. The value for the initial anisotropy, $r(0)$, was fixed at 0.376 while fitting the $r(t)$ for C153. The average rotational correlation time $\langle \tau_r \rangle$ was then determined as follows, $\langle \tau_r \rangle = \int_0^\infty dt[r(t)/r(0)] = a_1\tau_1 + (1-a_1)\tau_2$.

III. Results and Discussion:

IIIA. Steady State Spectral Properties: Signature of Heterogeneity

We measured steady state absorption and emission spectra of C153 in various DES with varying electrolyte and alkyl chain length of amide. Fig. 1 illustrates the representative absorption and emission spectra of C153 in DES made of CH_3CONH_2 with Na/KSCN, $LiNO_3$/Br ($f_{KSCN/LiBr}$ ~ 0.6) and $LiClO_4$ [17-20]. The spectral features of C153 in DES are almost similar to those obtained in formamide with respect to broadening and peak position. Therefore, these DES are not likely to possess a huge static dielectric constant ($\varepsilon_0 \sim 10^6$) as reported for a similar molten mixture via mega-hertz dielectric relaxation measurements [23] . The absorption and emission spectra exhibit peak position variation with electrolyte. While absorption frequency (ν_{abs}) shows a minimal effect with changing electrolyte, a marked electrolyte effect has been found in fluorescence, which displays ~ 500 cm^{-1} blue shift in frequency (ν_{em}) when NaSCN/KSCN is replaced by $LiNO_3$/LiBr at f = 0.6. The spectral features of {CH_3CONH_2 + NaSCN/KSCN} system are presented in Fig. 2. Absorption frequency (upper panel) and width (middle panel) show a non-monotonic KSCN concentration dependence but emission does not exhibit any change with KSCN comcentration[17]. The non-monotonicity is also reflected in KSCN concentration dependent relative ($\Delta\Delta\nu$) and estimated ($\Delta\nu_{est}(t)$) Stokes shift shown in the bottom panel of Fig. 2. This

non-monotonic alkali metal ion concentration dependence has also been found earlier in connection with transport property measurements and is known as mixed alkali effect (MAE)[6].

Now we will describe some temperature dependent spectral properties of ($RCONH_2$ + $LiClO_4$), where alkyl change length of amide has been varied from methyl (CH_3) to propyl ($CH_3CH_2CH_2$)[20]. From the frequency data of steady state and time resolved measurements in DES, we calculated solvation free energy difference, $\Delta G_s = 1/2\{h(\nu_{abs} + \nu_\infty)\} - \Delta G_0$ and reorganisation energy, $\lambda_s = 1/2\{h(\nu_0 - \nu_\infty)\}$ for $S_0 \leftrightarrow S_1$ transition of C153 following the reported method[14]. We have used an approximate gas phase value of $\Delta G_0 \cong 295.9$ kJmol^{-1} in conventional solvents. Fig. 3 shows the plots of $-\Delta G_s$ and λ_s as a function of temperature for three different types of mixtures. From the figure it is evident that the solvation energies do not exhibit much dependence (with in experimental error) as the alkyl chain length or temperature varied in molten mixtures. The calculated values of $-\Delta G_s$ and λ_s are much close to those obtained previously in many ionic liquids[14], indicating $S_0 \leftrightarrow S_1$ transition of C153 in these mixtures senses similar polar interactions as in those ionic liquids.

IIIB. Heterogeneity from Excitation Wavelength Dependent Study:

We explored the heterogeneous signature of DES by monitoring the excitation wavelength dependence.[19,20] We will describe excitation wavelength dependent behaviour of steady state fluorescence for two dipolar solute probes, C153 and DMASBT in DES composed of CH_3CONH_2 with $LiNO_3$, LiBr and $LiClO_4$. The measured fluorescence life times ($<\tau_{life}>$) of C153 is ~ 5 ns, whereas DMASBT exhibit a shorter life time ~ 0.5 ns in above DES at 303 K. Both of the solutes show $\lambda_{exc.}$ dependent fluorescence in these DES. In all the cases, shorter life time solute shows larger excitation wavelength dependence in both emission spectral frequency and width. The amount of emission frequency shift obtained from $\lambda_{exc.}$ dependence of fluorescence measurements for two solutes in these DES at 303 K is shown in Fig. 4. From the figure it is evident that the longer lifetime solute (C153) shows a lesser amount of shift whereas larger amount of shift has been detected in case of shorter lifetime solute (DMASBT). This $\lambda_{exc.}$ dependence of fluorescence behaviour clearly indicates that the mixtures possess heterogeneity. Such heterogeneity has been well documented in case of

ionic liquids, where solute life time played an important role in heterogeneity sensing [24]. Interestingly, the amount of shifts as exhibited by both the solutes are larger in case of $LiNO_3$ containing DES and smaller in $LiClO_4$ containing DES. Therefore the former may be termed as 'more heterogeneous' than the latter. The structure breaking ability of $ClO4^-$ ion might be a reason for the observed less pronounced $\lambda_{exc.}$ dependence. Eventhough any domain size or length scale over which the particle are correlated cannot be determined from these data, an idea about the lifetime of microscopic structures can be conjectured.

IIIC. Solvent Relaxation Dynamics from Time Resolved Stokes Shift Measurements:

We have extensively measured time resolved Stokes shift of C153 in (amide + electrolyte) DES with varying electrolyte, alkyl chain length and temperature. We have observed wavelength dependent fluorescence intensity decays in all the DES[17-20]. A fast decay at short wavelength and growth followed by decay at long wavelength (not shown here) indicated that solute undergo solvation in these DES. Minimal change of fluorescence lifetime was detected with variation of electrolyte/alkyl chain length or temperature in these DES. The time resolved emission spectra (TRES) have been synthesized following the literature method described in experimental section [21]. Acetamide DES in presence of Na/KSCN[17], estimated experimental dynamic Stokes shift ranges between ~1800 and ~ 2200 cm^{-1}, whereas in presence of $LiNO_3$/Br[19], it lies in the range, ~1000 – 1700 cm^{-1}. Interstingly, in presence of $LiClO_4$[20] estimated shift reduces to ~ 1000 cm^{-1} even with changing alkyl chain length of amide. Since we have employed a technique with broader time resolution (IRF ~70 ps), a significant portion of the total dynamic Stokes shift has been missed in many cases. We failed to detect nearly half of the total shifts in Li/KSCN[17] containing DES due to ultrafast dynamic response of solvent which is faster than experimental time resolution. Comparatively lesser amount of total dynamic shifts have been missed in LiNO3/Br[19] containing DES, where higher viscosity might be responsible factor for the observed fact. Most interestingly, percentage of missing components in DES made of ($RCONH_2$ + $LiClO_4$) with varying alkyl chain length are much smaller, even in many cases it is zero[20]. This fact clearly indicates medium dynamics has been governed differently in presence of ClO_4^- ion. One point to be mentioned here is that amide systems are known to possess collective librational modes at ~100 cm^{-1} (due to intermolecular H-bonding)[25] and these modes are participated in ultrafast solvation response[26]. There has been a possibility

of complex formation (H-bond formation) between ClO_4^- anion and amide and thereby reducing the ability of collective intermolecular H-bond formation between amide molecules. This complexing ability of ClO_4^- ion with amide molecules from producing a collective H-bonding network is termed here as structure breaking ability [27].

Steady state fluorescence spectrum in all the systems have been found to be ~500 – 700 cm^{-1} 'blue shifted' compared to $t = \infty$ spectra[17-20]. This indicates that the steady state fluorescence does not come from the completely environment relaxed state due to presence of dipole-ion composite species in these DES and closely resembles to the findings in ionic liquids. It is long known that acetamide aggregates in presence of ion, sometimes referred to polymerized amide forming various domain.[5,12] The red shifted $t = \infty$ spectra compared to steady state spectra possibly observed in these DES due to presence of heterogeneous solution structure.

Representative decay of the solvation response function, $S(t)$, at 318 K obtained from the time resolved emission spectra are shown in Fig 5. The effects of cation and anion are shown in the upper and lower panels, respectively. The figure clearly indicates that $S(t)$ decays sense ion identity[17-20] as the physico-chemical properties of a solution also depend on nature of electrolyte[6]. The decay of $S(t)$ becomes faster when Na^+ is replaced by K^+ in (CH_3CONH_2 + Na/KSCN) melt (upper panel). This correlates well with the decrease in medium viscosity in presence of K^+. In DES composed of acetamide with lithium salt, $S(t)$ also follow the viscosity trend of the medium.

Now we will discuss the dependence of average solvation time, $<\tau_s>$ of C153 on the medium viscosity (η) in DES which is an important physical parameter for the dynamics in liquids[17-20,28]. Fig. 6 shows the $<\tau_s>$ versus temperature reduced viscosity (η/T) for (acetamide + electrolyte) DES with varying electrolyte. From the Fig. 6, it is clearly observed that a power-law dependence of $<\tau_s>$ on η/T, $<\tau_s> = A(\eta/T)^p$, with a fractional power less than unity (p = *0.57*, *0.43* and *0.37* for $LiClO_4$, $LiNO_3$ and LiBr respectively)[19,20] in all the cases. This description suggests presence of pronounced heterogeneity in these DES. In other sense, the average solvation time is governed by spatial diffusional motion of particle (in the present systems ion-induced polymerised amide) this is associated to the long time

constant of $S(t)$ decay. Therefore, Stokes-Einstein (SE) relation is not sufficient in this case. Strong microscopic heterogeneity in DES forbids Brownian motion of the particles as envisaged while deriving these hydrodynamic relations for a solute in a homogeneous medium. Therefore, indirectly the value of *p* (the extent of coupling) could be a measure of decoupling arising from medium heterogeneity. It is also evident from the figure that, decoupling is large in presence of LiBr and small in presence of $LiClO_4$. Hence, ClO_4^- containing DES is less heterogeneous which is possibly due to structure breaking ability of ClO_4^- ion[27]. We also observed earlier that the ClO_4^- containing DES so less amount emission spectral shift with $\lambda_{exc.}$ This is in accordance with the lesser decoupling observed for relaxation rates.

IIID. Solute Rotational Dynamics and Viscosity Decoupling:

Representative fluorescence anisotropy decay for (CH_3CONH_2 + $LiNO_3$)[19] DES at 303 K is shown in Fig. 7. The bi-exponential fitted line through the data points and the relevant fit parameters are also shown in the same figure. The value for the initial anisotropy ($r(0)$) of C153 was fixed at 0.376 for all samples at all temperatures. The corresponding residual of the fitting is shown in the bottom panel of the figure. To check the validity of hydrodynamic relation for solute rotation, we have plotted average rotation time, $\langle \tau_r \rangle$, as a function of temperature-reduced viscosity (η / T) for $LiNO_3$, LiBr and $LiClO_4$ containing DES in Fig. 8. It shows a power law dependence, $\langle \tau_r \rangle \propto (\eta / T)^p$, as found in solvation measurements. The observed decoupling of solute rotation is then mediated by the temporal heterogeneity of DES. Like in solvation, the fraction power, '*p*', found to be dependent on the nature of electrolyte. LiBr containing DES shows greater decoupling, whereas presence of $LiClO_4$ leads to lesser decoupling[20] due to structure breaking ability of ClO_4^- ion. Another important point to note here that the values of '*p*' obtained in solvation dynamics measurements are smaller compared to those obtained solute relaxation dynamics. So there has been a short of translation-rotational decoupling which has been observed earlier in deeply supercooled liquids [29].

IV. Conclusions:

To summarize, the present study involving DES reveals presence of both spatial and temporal heterogeneities which induce fractional viscosity dependence of the rates of solute-centred relaxation dynamics in these media. In addition, the extent of heterogeneity depends on ion identity as excitation wavelength dependence of emission frequency and viscosity-decoupling changes as one electrolyte is replaced by another. Further experiments, especially X-ray and neutron scattering experiments are required to fully ascertain the spatial correlations present in these DES. All-atom simulations may also help in this direction.

Acknowledgement

BG thanks the CSIR for a research fellowship.

References:

1. van Rantwijk, F.; Sheldon, R. A. *Chem. Rev.* **2007**, *107*, 2757.
2. Noyori, R. (Ed.) *Chem. Rev.* **1999**, *99*, 353-354.
3. Hurley, *J. Electrochem. Soc.*, **1951**, *98*, 207.
4. Abbott, A. P.; Boothby, D.; Capper, G.; Davies, D. L.; Rasheed, R. K. *J. Am. Chem. Soc.* **2004**, *126*, 9142.
5. Berchiesi, G. *J. Mol. Liq.*, **1999**, *83*, 271.
6. Kalita, G.; Rohman, N.; Mahiuddin, S. *J. Chem. Eng. Data* **1998**, *43*, 148.
7. Jin, H.; O'Hare, B.; Dong, J.; Arzhantsev, S.; Baker, G. A.; Wishart, J. F.; Benesi, A. J.; Maroncelli, M. *J. Phys. Chem. B*, **2007**, *112*, 81-92.
8. Kerridge, D. H. *Chem. Soc. Rev.* **1988**, *17*, 181.
9. Chen, R.; Wu, F.; Xu, B.; Li, L.; Qiu, X.; Chen, S. *J. Electrochem. Soc.*, **2007**, *154*, A703.
10. Dhanalakshmi, K.; Saraswathi, R.; Srinivasan, C. *Synth. Met.*, **1996**, *82*, 237.
11. Venkata Narayanan, N.S.; Ashokraj, B.V.; Sampath, S. *Electrochem. Commun.*, **2009**, *11*, 2027–2031.
12. Berchiesi, G.; Rafaiani, G.; Vitali, G.; Farhat, F. *J. Therm. Anal*. **1995**, *44*, 1313.
13. Karmakar, R.; Samanta, A. *J. Phys. Chem. A* **2002**, *106*, 4447.
14. Jin, H.; Baker, G. A.; Arzhantsev, S.; Dong, J.; Maroncelli, M. *J. Phys. Chem. B* **2007**, *111*, 7291.
15. Chakrabarty, D.; Chakraborty, A.; Seth, D.; Sarkar, N. *J. Phys. Chem. A* **2005**, *109*, 1764.
16. Kashyap, H. Biswas, R. *J. Phys. Chem. B*, **2010**, ***114***, 16811.
17. Guchhait, B.; Gazi, H. G.; Kashyap, H. Biswas, R. *J. Phys. Chem. B*, **2010**, *114*, 5066.
18. Gazi, H. R.; Guchhait, B.; Daschakraborty, S.; Biswas, R. *Chem. Phys. Lett.* **2011**, *501*, 358.
19. Guchhait, B.; Daschakraborty, S.; Biswas, R. *J. Chem. Phys.* **2012**, *136*, 174503.
20. B. Guchhait, S. Daschakraborty and R. Biswas, *J. Phys. Chem. B*, **2013**, (submitted).
21. Horng, M. L.; Gardecki, J. A.; Papazyan, A.; Maroncelli, M. *J. Phys. Chem.* **1995**, *99*, 17311.
22. Horng, M. L.; Gardecki, J. A.; Maroncelli, M. *J. Phys. Chem. A* **1997**, *101*, 1030.

23. Amico, A.; Berchiesi, G.; Cametti, C.; Biasio, A. D. *J. Chem. Soc. Faraday Trans. 2*, **1987**, *83*, 619.
24. Samanta, A. *J. Phys. Chem. B*, **2006**, *110*, 13704-13716.
25. Shirota, H.; Castner, E. W. Jr. *J. Am. Chem. Soc.* **2001**, *123*, 12877-12885.
26. Biswas, R.; Bagchi, B. *J. Phys. Chem.* **1996**, *100*, 1238-1245.
27. Bondarenko, G. V.; Gorbaty, Y. E. *Mol. Phys.* **2011**, *109*, 783-788.
28. Bagchi, B.; Biswas, R. *Adv. Chem. Phys.* **1999**, *109*, 207.
29. Ediger, M. D. *Annu. Rev. Phys. Chem.* **2000**, *51*, 99.

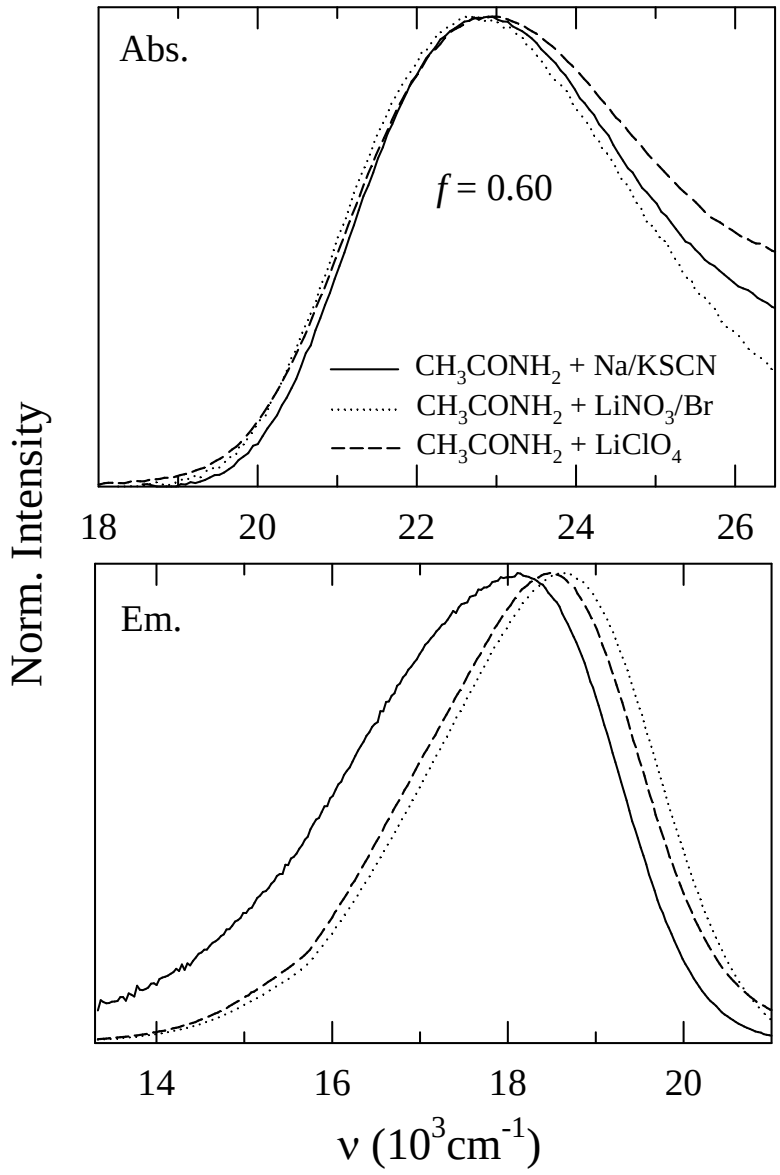

Fig. 1: Representative steady-state absorption (upper panel) and emission spectra (lower panel) of C153 in acetamide DES, where solid, dotted and dashed lines represent [0.75CH_3CONH_2 + 0.25{*f*KSCN + (1-*f*)KSCN}], [0.78CH_3CONH_2 + 0.22{*f*LiBr + (1-*f*)$LiNO_3$}] at $f = 0.6$ and [0.81CH_3CONH_2 + 0.19$LiClO_4$] DES respectively.

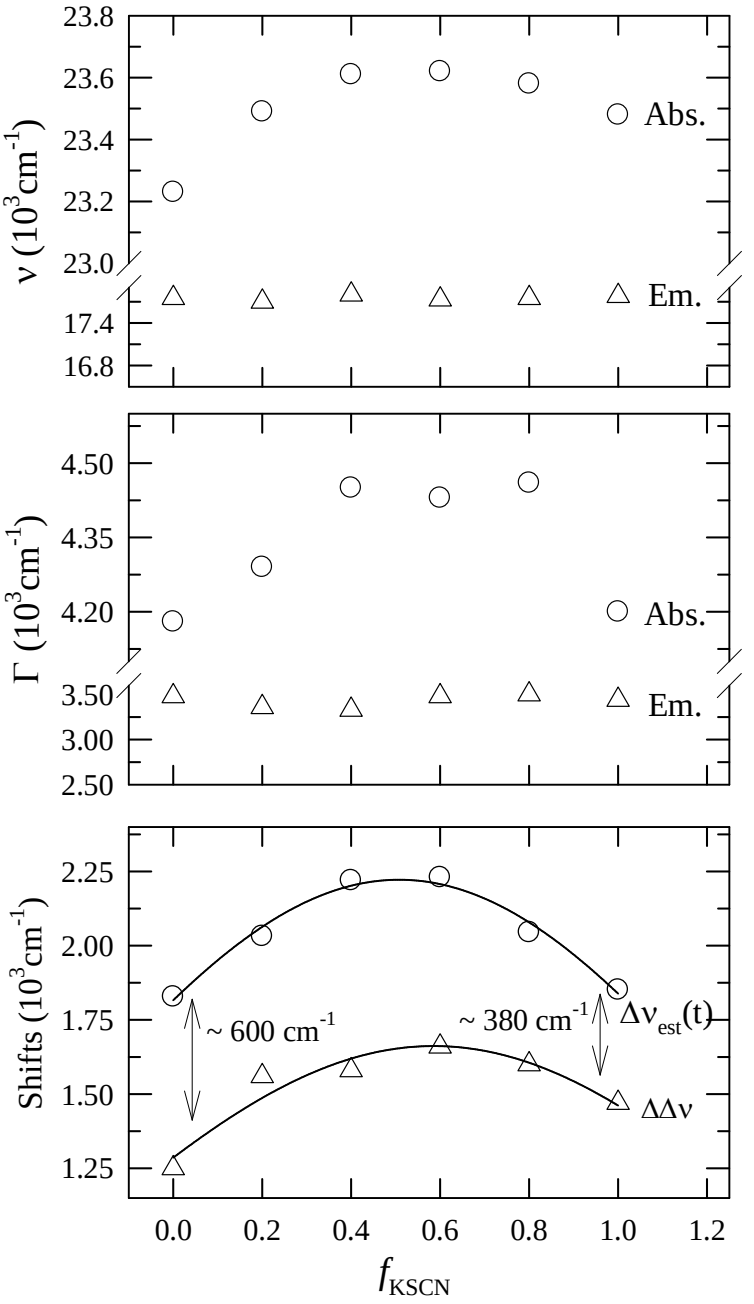

Fig. 2: *f* dependent spectral properties of C153 in [0.75CH_3CONH_2 + 0.25{*f*KSCN + (1-*f*)KSCN}] DES. Spectral frequencies (ν), full-width-at-half-maxima (Γ) and Stokes shifts (relative, $\Delta\Delta\nu$ and estimated, $\Delta\nu_{est}(t)$) are shown in upper, middle and lower panel respectively.

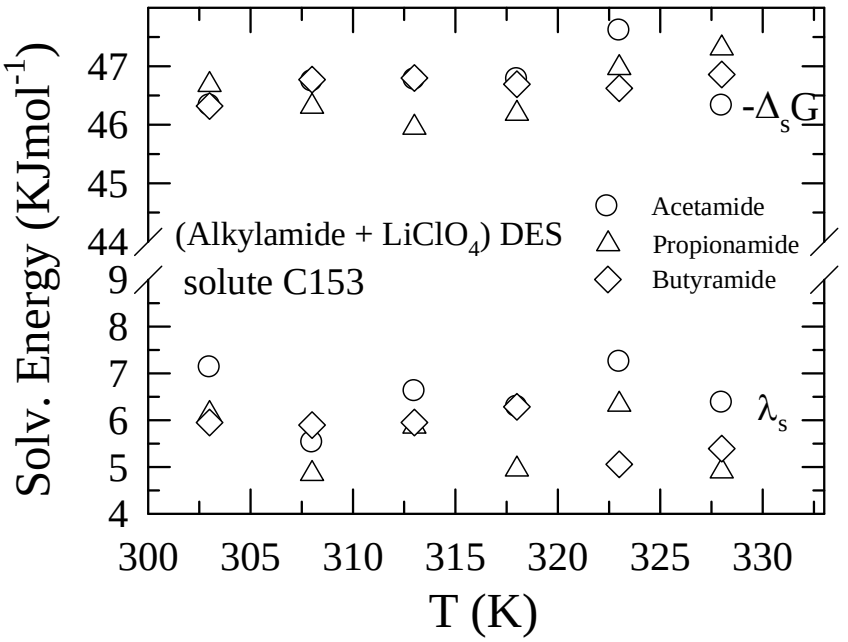

Fig. 3: Solvation energies ($-\Delta_s G$ and λ_s) of C153 as a function of temperature in ($0.81RCONH_2 + 0.19LiClO_4$) DES. The two types of solvation energies, free energy ($-\Delta_s G$) and reorganisation energy (λ_s) are defined in the text.

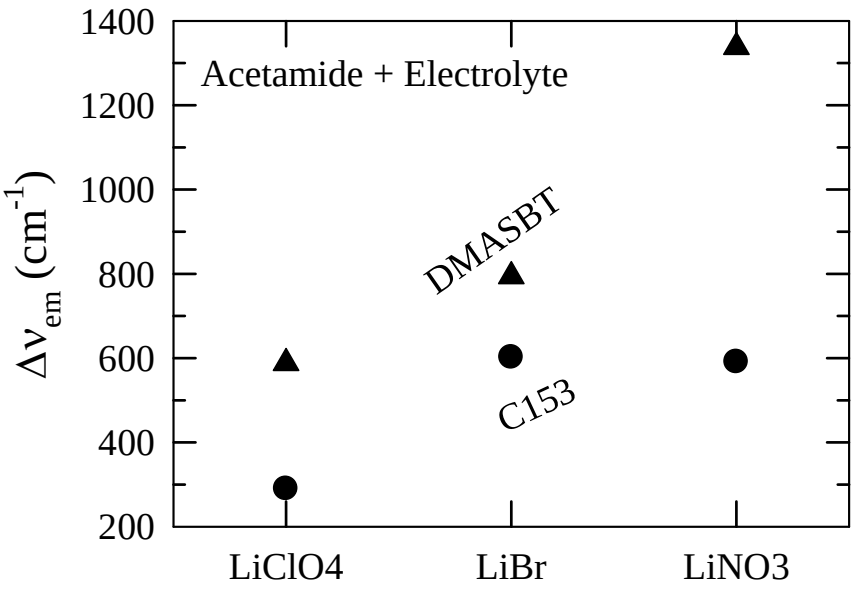

Fig. 4: Total amount of shift ($\Delta\nu$) in emission frequency of C153 and DMASBT obtained from $\lambda_{exc.}$ dependent measurement in $LiNO_3$, LiBr and $LiClO_4$ contaning acetamide DES. $\Delta\nu$ is defined as: $\Delta\nu = \nu(\lambda_{exc.,b}) - \nu(\lambda_{exc.,r})$, where $\lambda_{exc.,b}$ and $\lambda_{exc.,r}$ are the shortest and longest wavelengths used for solute excitation. The values are better than $\pm$ 200 cm^{-1}.

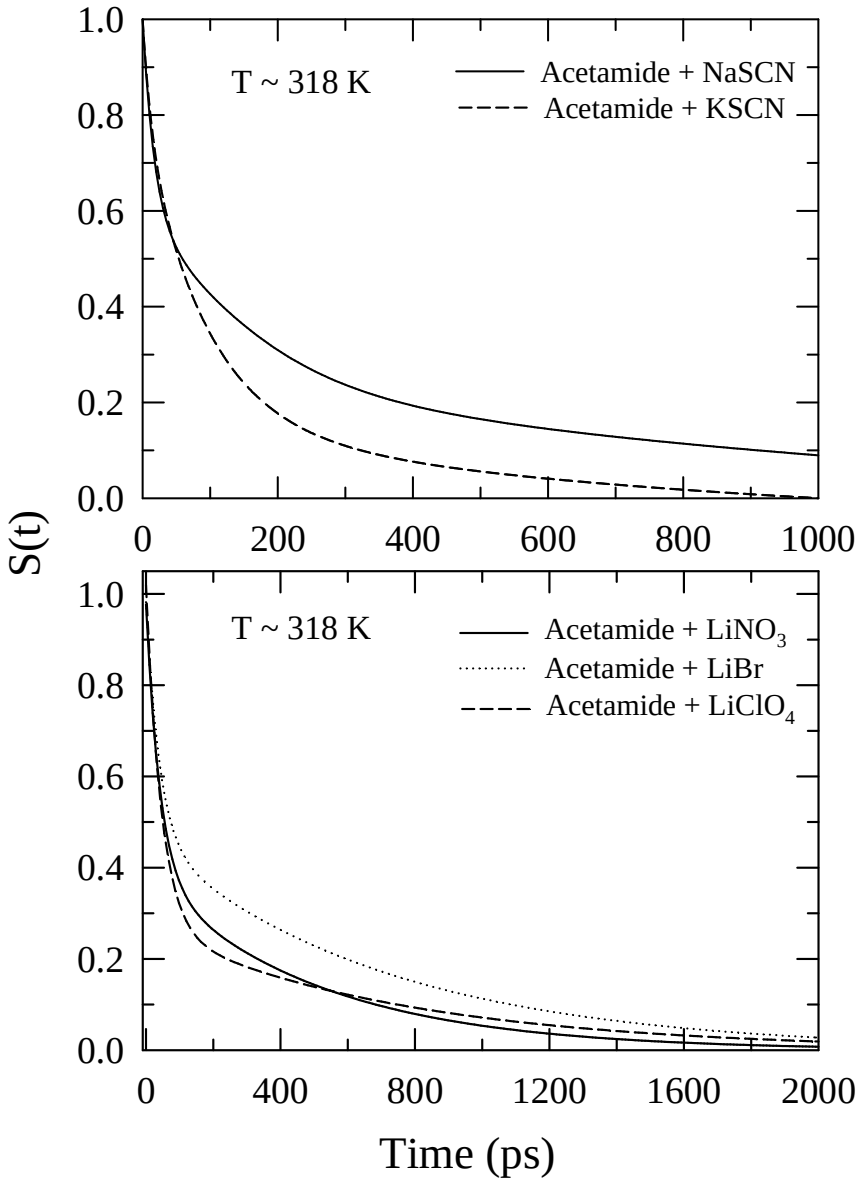

Fig. 5: Decays of solvent response function, $S(t)$ of C153 in NaSCN and KSCN containing DES (upper panel), and $LiNO_3$, LiBr and $LiClO_4$ containing DES (lower panel) at 318 K.

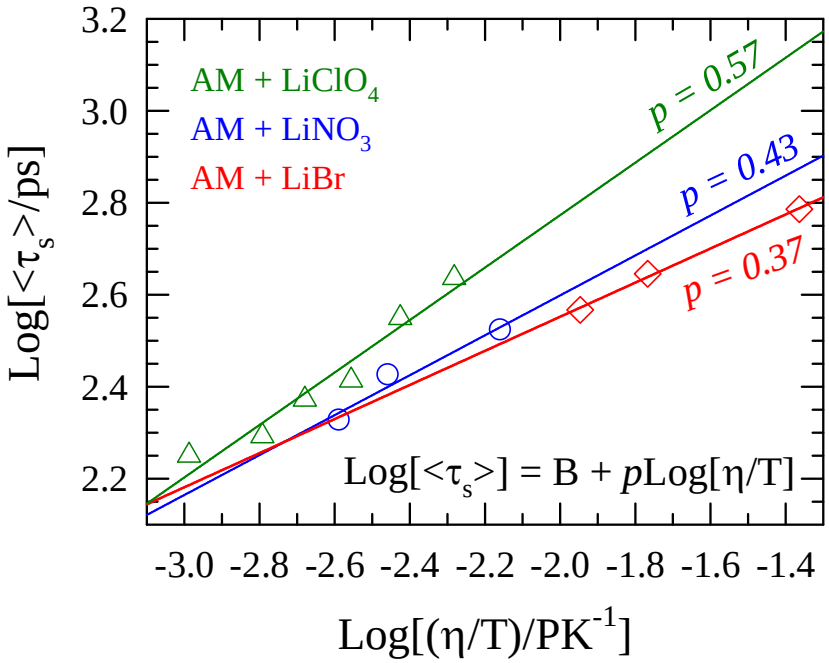

Fig. 6: Log-Log plot of average solvation time, $<\tau_s>$ of C153 versus η/T in (acetamide + electrolyte) DES, where AM stands for acetamide. Blue circles, red diamonds and green triangles represent data in LiNO3, LiBr and $LiClO_4$ containing DES. The solid lines show the best fits of the experimentally measured data to the relation $Log[<\tau_s>] = B + pLog[\eta/T]$, the associated *p* values are given in the figure.

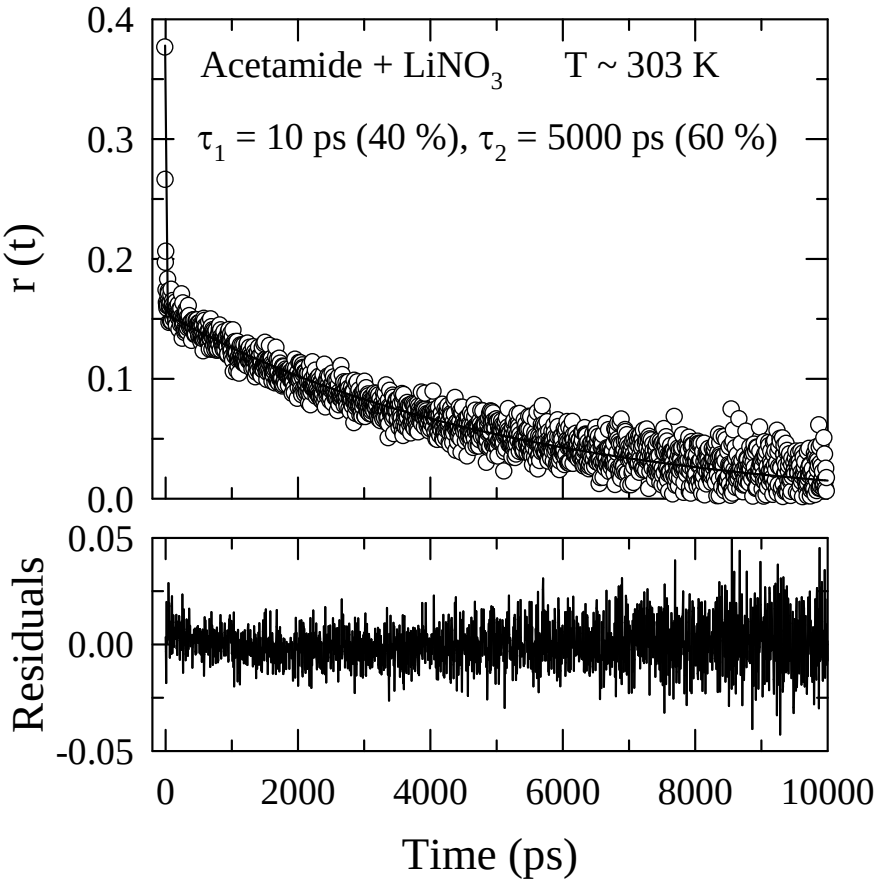

Fig. 7: Representative fluorescence anisotropy decay, $r(t)$, of C153 at ~303 K in $LiNO_3$ containing acetamide DES. Circles represent experimental decay in the upper panel and the solid line denotes the fit through them. The fit parameters are shown in the inset. Bottom panel shows the residuals.

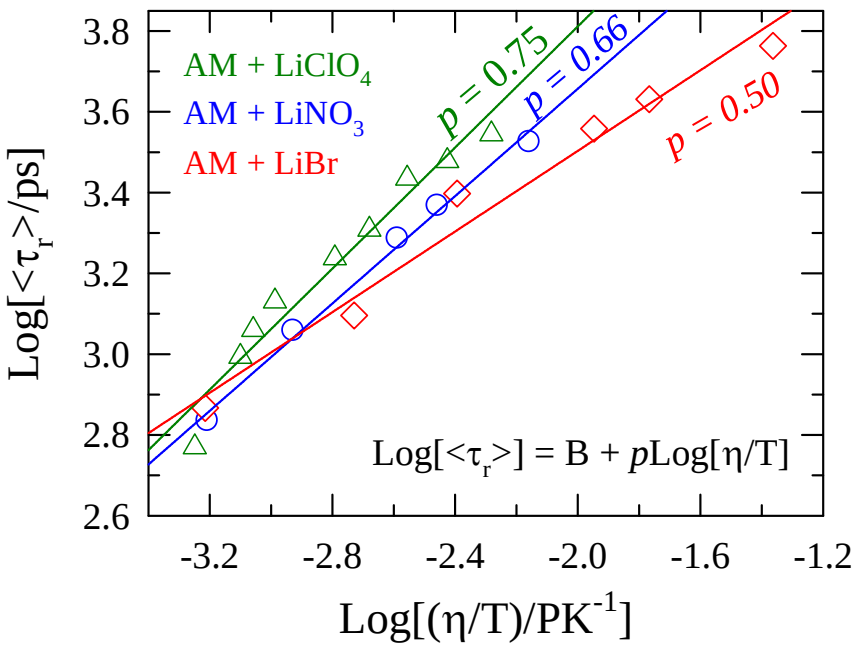

Fig. 8: Log-Log plot of average rotational correlation time, $<\tau_r>$ of C153 versus η/T in (acetamide + electrolyte) DES, where AM stand for acetamide. Blue circles, red diamonds and green triangles represent data in $LiNO_3$, LiBr and $LiClO_4$ containing DES. The solid lines show the best fits of the experimentally measured data to the relation $Log[<\tau_r>] = B + pLog[\eta/T]$, the associated *p* values are given in the figure.